Long-Term Stability of the NIST Chip-Scale Atomic Clock Physics Packages

S. Knappe*[1], V. Gerginov[2], V. Shah[3], A. Brannon[4], L. Hollberg[1], J. Kitching[1]

[1]NIST, Time and Frequency Division, Boulder, CO 80305
[2]Department of Physics, University of Notre Dame, Notre Dame, IN 46556
[3]Department of Physics, University of Colorado, Boulder, CO 80309
[4]Department of Electrical Engineering, University of Colorado, Boulder, CO 80309

ABSTRACT

We discuss the long-term stability of the NIST chip-scale atomic clock (CSAC) physics packages. We identify the major factors that currently limit the frequency stability of our CSAC packages after 100 s. The requirements for the stability of the vapor cell and laser temperature, local magnetic field, and local oscillator output power are evaluated. Due to the small size of CSAC physics package assemblies, advances MEMS packaging techniques for vacuum sealing and thermal isolation can be used to achieve the temperature stability goals. We discuss various ideas on how to aid temperature control solutions over wide variations in ambient temperature by implementing atom-based stabilization schemes. Control of environment-related frequency instabilities will be critical for successful insertion of CSACs into portable instruments in the areas of navigation and communication.

Keywords: atomic clock, coherent population trapping, CPT, CSAC, MEMS, microfabrication

1. INTRODUCTION

Chip-scale atomic clocks (CSACs) have rapidly advanced since their proposal in 2001[1]. The combination of MEMS fabrication techniques and atomic physics has led to the development of small, low cost atomic clocks with much reduced power consumption. Embedding these clocks in battery-operated portable devices would have many potential applications in the telecommunication and navigation sector[2-5]. After the initial demonstration of the first microfabricated alkali vapor cells[6] and CSAC physics packages[7], many improvements have been made in terms of short-term frequency stability[8], power consumption[9], and size[10]. Low-power local oscillators have been developed[11-13] and integrated onto the same substrate as the physics package[14].

Our CSACs are based on coherent population trapping (CPT) spectroscopy[15] of ^{87}Rb atoms confined in a vapor cell. Here a vertical-cavity surface-emitting laser (VCSEL) is tuned to the D_1 transition of ^{87}Rb at 795 nm. A voltage-controlled oscillator (LO) with an output frequency near 3.4 GHz modulates the injection current of the VCSEL and creates modulation sidebands around the carrier. If the beat frequency between the two first-order sidebands is exactly resonant with the ground-state hyperfine splitting of the ^{87}Rb atoms at 6.8 GHz, the light absorbed by the atoms decreases. This CPT resonance can have a quality factor (Q) as high as 3 million and can be used to stabilize the frequency of the local oscillator. A schematic of such a clock is shown in Fig. 1.

* knappe@boulder.nist.gov: phone 1 303 497-3334

MOEMS and Miniaturized Systems VI, edited by David L. Dickensheets, Bishnu P. Gogoi, Harald Schenk, Proc. of SPIE Vol. 6466, 64660O, (2007) · 0277-786X/07/$15 · doi: 10.1117/12.701591

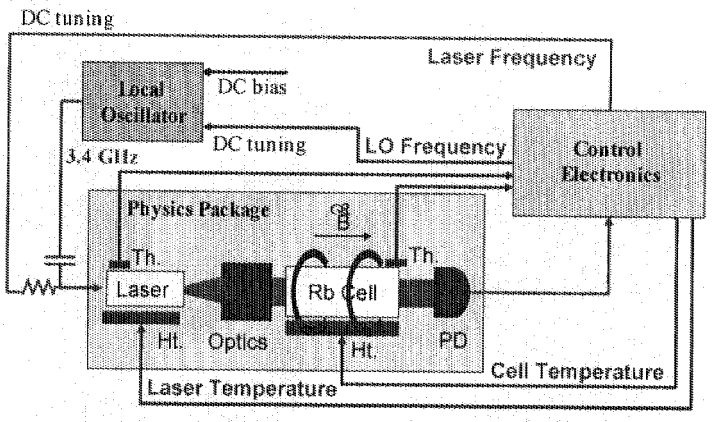

Fig. 1. Schematic of a chip-scale atomic clock. Four control loops are implemented by control electronics. The clock signal derived from the atoms is used to stabilize the LO frequency. The laser frequency is stabilized to the atomic absorption (green circuit). The laser and cell temperatures are stabilized by use of thermistors Th. and heaters Ht. (blue circuits). The local oscillator modulates the laser injection current and is stabilized to the atomic transition through the signal from the photodetector PD (red circuit).

In a microfabricated device, the atoms are confined inside a MEMS vapor cell[6] along with a buffer gas. To achieve enough absorption of the laser light, the cell must be heated to approximately 90 °C. Furthermore, the laser frequency must be stabilized, usually by controlling the laser temperature and DC injection current. The light is attenuated, its polarization controlled, and the power transmitted though the cell detected by a photodiode. The components of the physics package that make up the atomic spectrometer can be seen in Fig 2. The local oscillator (see Fig. 1) is based on a coaxial resonator with an unloaded Q of 125 and generates a 3.4 GHz output signal with a power of -6 dBm, enough to sufficiently modulate the VCSEL[13]. The microwave output power is controlled by a DC bias and its frequency is steered with a DC voltage, derived from the atomic CPT resonance signal. In a system that combined this type of low-power LO and physics package, clock stabilities of $2 \times 10^{-10}/\tau^{1/2}$ have been achieved.

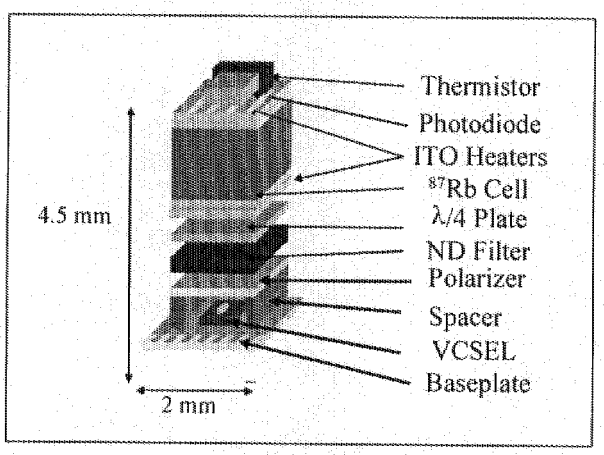

Fig. 2. Chip-scale atomic clock physics package. The VCSEL is mounted onto a baseplate so that it emits vertically. The optics package for shaping the light beam consists of a polarizer, a quarter waveplate, and neutral density (ND) filters. The atoms are confined inside a MEMS vapor cell heated to 90 °C by two pairs of heaters and temperature stabilized by use of a thermistor. The photodetector on top detects the light transmitted through the atomic vapor.

Despite of extensive characterization of the short-term frequency stability, relatively little has been reported on the frequency stability of these clocks at integration periods beyond several minutes. Many applications demand frequency stabilities near 1×10^{-11} at integration periods of 1 hour and longer. With short-term instabilities below $6 \times 10^{-10}/\tau^{1/2}$, this should be achievable, if white frequency noise dominates the instability. In practice frequency drifts limit the stability at longer periods. Fig. 3 shows typical frequency stabilities as a function of averaging periods of several clock components. The green diamonds show the instability of the free-running local oscillator, which begins to drift after only a few second[13]. The blue triangles show the instability of the hyperfine transition of rubidium atoms confined in a MEMS vapor cell similar to ones integrated in the CSACs[16]. In a laboratory environment, these cells can support instabilities below 10^{-11} at 1 hour of integration. The red dots correspond to a CSAC physics package alone run with a commercial synthesizer[8], and the black squares show the frequency instability of a CSAC physics package integrated with a local oscillator[13]. In the following sections we will discuss the factors that cause the frequency drifts in our devices and discuss possible improvements.

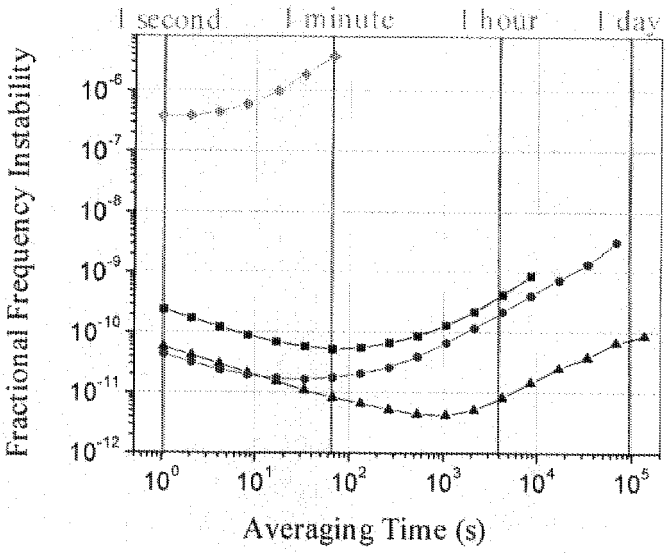

Fig. 3. Fractional frequency instabilities of chip-scale atomic clock components as a function of averaging period: free-running low-power 3.4 GHz oscillator (green diamonds), MEMS vapor cell (blue triangles), CSAC physics package (red dots), CSAC physics package and local oscillator integrated (black squares).

2. CELL TEMPERATURE

Temperature-induced shifts of the resonance frequency of alkali atoms in vapor cells have been known for many decades. In most systems, they arise from the collisions of the alkali atoms with the so-called buffer gases. These buffer gases are mostly inert or molecular gases that interact only weakly with alkalis, and cause the alkalis to diffuse slowly through the cell, reducing the frequency of wall collisions. As a result, the lifetime of the coherence in the atoms is increased and narrower resonance lines are achieved. Despite the weak interaction between the buffer gas and the alkali atoms, some shifts in the resonance frequency do occur, and these depend on the temperature of the gases. Heavy buffer gases (Ar, Xe, CH_4,...) shift the clock frequency to negative values with increasing temperature, while light buffer gases (Ne, N_2,...) result in a positive temperature coefficient. Therefore, in commercial rubidium vapor cell clocks, combinations of two buffer gases are often used to cancel the temperature-dependent shift to first order[17, 18]. In this way, temperature-induced shifts on the order of $-2 \times 10^{-12}/\,°C^2$ are achieved in cells a few centimeters in size. In millimeter-sized cells, the buffer gas pressures are usually an order of magnitude higher, resulting in proportionally higher temperature-induced shifts. Cell temperature stabilities below 1°C should be

sufficient to support clock stabilities around 10^{-11}, if it were possible to achieve buffer gas pressure ratios with the same accuracy as in larger glass-blown cells.

Precise adjustment of the buffer gas pressure ratio is complicated by the fabrication methods of MEMS cells. Most methods use anodic bonding to seal the cell, and chemical byproducts are created during bonding. With typical clock frequency shifts on the order of 8×10^{-11}/(Torr °C), the residual gases produced during bonding should be less than 100 mTorr in pressure to achieve stabilities below 10^{-11} with 1 °C temperature stability. We have found, however, that in our cell fabrication apparatus, it is difficult to reduce the residual pressure in the final cell to below 1 Torr, even when the wafers are baked under vacuum at 300 °C for 12 hours prior to filling the cells and background pressures inside the vacuum chamber at 10^{-6} Torr during bonding. Therefore, the temperature coefficient of our vapor cells is usually around ~4 Hz/K (or 6×10^{-10}/K). Such temperature coefficients require a temperature stability around 20 mK to ensure a frequency stability of 10^{-11}.

Temperature stabilities of 20 mK can be reached with fairly simple electronic servos in laboratory environments, and it has been shown that microfabricated vapor cells can support clock frequency stabilities of 5×10^{-12} at 1000 s of averaging periods in table-top setups. In small CSAC physics packages suitable for field use however, this temperature stability must be maintained over the whole ambient temperature range often more than 70 °C. In our devices, we found that we are unable to reach these wide operating ranges when using thermistors separated from the cell by a distance of ~500 μm to measure the cell temperature[19]. This is because the temperature gradient between cell and thermistor varies with the ambient temperature and hence even when the thermistor temperature is stabilized precisely, the cell temperature may show significant deviations. One solution to this problem, for example, is to stabilize the cell temperature by maintaining a constant optical DC absorption[19]. This stabilizes the atom density inside the cell instead of the temperature of the cell body and ensures much better temperature stability when the ambient temperature is changing.

3. LASER TEMPERATURE

The temperature of the VCSEL is even more critical than the cell temperature. The optical frequency of these lasers tunes with temperature and current by 30 GHz/K and 300 GHz/mA, respectively. To keep the laser frequency resonant with the atomic transition, the laser temperature is usually monitored with a thermistor and stabilized by feeding back to the local heater. The laser current is then modulated and the power transmitted through the cell is detected at the modulation frequency. This signal can then be used to stabilize the laser frequency to the center of the atomic absorption line. Similarly to the problems with the cell temperature, temperature gradients between thermistor and laser will change the laser temperature if the ambient temperature is changing. Even if the laser frequency remains the same because of the servos, the total laser power will change due to a different operating current. This coefficient is ~30 μW/K for our VCSELs. This results in a change of total light power at the cell of ~1 μW/K (for a total power of 10 μW) after attenuation in the optics assembly, and leads to clock frequency shifts of $\sim 5 \times 10^{-9}$/K. Thus, maintaining a frequency stability of 10^{-11} would require an absolute laser temperature stability of ~2 mK. With the thermistor technique currently used, this is not possible over a wide range of ambient temperatures. With better thermal design (like the one developed by R. Lutwak et al.[9], for example) the temperature shifts could be reduced, but it would probably still be challenging to ensure the required stability over more than 70 °C of ambient temperature change. Most commercially available rubidium vapor cell clocks use a lamp as the light source and do not need to address this problem.

Several spectroscopic techniques have been proposed to circumvent the laser-temperature-related instabilities. The clock frequency shift arises from the AC Stark shifts due to all laser sidebands and is therefore dependent on light powers and detunings of all those sidebands. It has been shown that it is possible is to operate at a point where the light-induced frequency shifts from all modulation sidebands mutually cancel[20-22]. In order to so that, the modulation index of the light fields must be chosen carefully and depends on the characteristics of the laser. It has been demonstrated that this technique also works well

in MEMS clock cells with high buffer gas pressures[23]. Nevertheless, it can be challenging to select all the operating parameters simultaneously in a small compact device, and this method works only in a narrow region of temperatures and powers. However, it has been shown in a table-top setup that the light modulation index can be *actively* stabilized to the point where all the light shifts cancel, by modulating the light power with a liquid-crystal modulator[24]. The shift of the clock frequency that is in phase with this modulation can then be used to stabilize the sideband strength of the light field to the point of minimal light shift. In a different method, the laser DC current is kept constant, using a constant current source, ensuring a stable total light intensity[19]. The laser frequency is then locked onto the optical absorption resonance by AC modulating the laser current and monitoring the modulation on the light transmitted through the cell. This signal is then used to correct the laser temperature with a bandwidth of 30 Hz. All of these methods have been shown to greatly improve the temperature stability of the clock frequency, but it is not yet known whether they are sufficient to reach clock frequency stabilities of 10^{-11} over the full range of ambient temperatures.

4. LOCAL OSCILLATOR OUTPUT POWER

In the previous section we mentioned that the clock output frequency depends on the light power in each one of the optical sidebands. While the total light power is determined by the laser current, the distribution of light power among the modulation sidebands is determined by the FM modulation index, which is related to the RF output power of the local oscillator and how much of this power is coupled into the VCSEL. We have observed the importance of maintaining a constant modulation index to ensure a stable clock frequency. In one of our table-top systems, we measured the overall system frequency shift as ~2 × 10^{-10}/mW RF power around 10 dBm output power from the LO[23]. The modulation index of the light field can also change if the VCSEL RF impedance changes with temperature, bias current, and aging. The overall result is a light-induced frequency shift that will perturb the clock frequency. We found that this change in laser impedance has an even more serious effect in a small CSAC system. As shown in Fig. 4, the VSCEL and the LO are mounted on the same substrate in order to maximize the coupling of the 3.4 GHz modulation into the VCSEL. In this particular case, 0.25 mW of power is sufficient to modulate the VCSEL at its optimum modulation index. As the impedance of the VCSEL changes with temperature, both the RF power and the reflections back into the oscillator change. This causes a complicated interplay that can shift the clock frequency dramatically and can sometimes degrade the stability by orders of magnitude when it pushes the LO into a multimode regime[14].

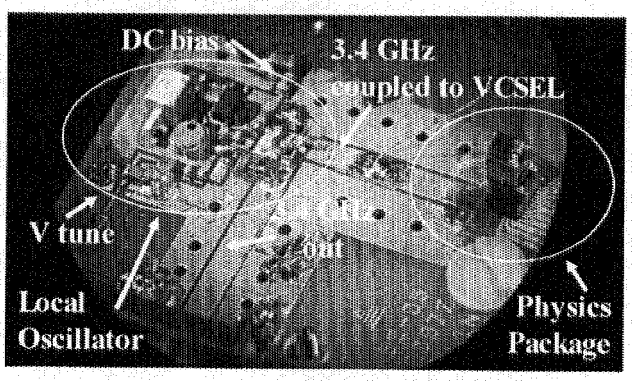

Fig. 4. Photograph of an integrated chip-scale atomic clock local oscillator (left) and physics package (right). The LO output signal is coupled directly to the VSCEL in the physics package. The control electronics use the photodiode output signal from the physics package to steer the local oscillator though the DC tuning port.

To reduce the problem of clock frequency shifts due to changes in the modulation power, some of the stabilization techniques introduced in the previous section can be useful. When the VCSEL is run with a constant current, its impedance is much more stable and it becomes possible to impedance match the

VCSEL to the output of the local oscillator, allowing both efficient coupling and a more stable output power[19]. The LO output power could then be stabilized with active feedback from the photodetector to the LO bias voltage to maximize the power in the first-order modulation sidebands of the laser, by modulating this power, for example, through the LO bias and phase-sensitive detection of this modulation in the light transmitted though the atomic vapor[19]. As another alternative, the LO power could be changed continuously to actively stabilize the modulation index to the point where the light-induced clock frequency shifts are minimal[24]. In addition, adding a second-stage buffer after the output of the LO would reduce the oscillator's frequency pulling sensitivity[14].

5. MAGNETIC FIELDS

In order to excite CPT "clock" resonances with circularly-polarized light, a magnetic bias field must be applied oriented along the direction of propagation of the light field. This field separates the magnetically-sensitive transitions from the magnetically insensitive "clock" transition and eliminates the linear shift in the resonance frequency with magnetic field (linear Zeeman shift). However, a second order contribution remains, which shifts the resonance by $\gamma = 8\times 10^{-12}/\mu T^2$. In the presence of the DC bias field B_{0z}, this second order shift results in a first-order dependence on changes ΔB_z in the bias field if $\Delta B_z \parallel B_{0z}$ ($\Delta f = \gamma B^2 = \gamma(B_{0z}+\Delta B_z)^2 \cong \gamma(B_{0z}^2 + 2B_{0z}\Delta B_z)$) and a second-order dependence on changes ΔB_x if $\Delta B_x \perp B_{0z}$ ($\Delta f = \gamma B^2 = \gamma(B_{0z}^2+\Delta B_x^2)$).

The frequency shifts discussed in the previous sections were caused mostly by ambient temperature changes. To a large extent they could be minimized with the addition of stabilization loops (for the RF power or total light power, for example) that use parameters directly derived from the atomic spectroscopy. There is also a magnetic field-induced frequency shift that is indirectly related to environmental temperature changes, but it could be reduced by a better thermal design and shielding. Typically, our cell heaters contribute the strongest magnetic fields at the location of the atomic vapor cell. As can be seen in Fig. 2, the heaters are thin conductive layer of indium-tin oxide (ITO) deposited on transparent glass substrates that are placed back-to-back on both sides of the vapor cell. The heater on each side of the cell consists in turn of two such 200 μm thick sheets with the current traveling in opposite directions to significantly cancel the magnetic fields produced by the sheets. The current is delivered from the baseplate below the CSAC physics package to the heaters by means of gold wires. In our design, 30 mA of current flows through the heaters to maintain the required cell temperature, so that a wire produces a magnetic field of roughly 6 μT at a distance of 1 mm. The major component of this field is perpendicular to the laser beam. In order to excite the CPT resonance between the hyperfine energy levels, which are shifting in second order with magnetic field only, a magnetic field parallel to the laser beam is needed. We therefore apply an external offset field of at least 60 μT along the direction of the laser beam, to ensure a total field direction close to this.

The clock transition has a second-order frequency shift with magnetic field of $8 \times 10^{-12}/\mu T^2$. In our offset field this translates into a shift rate of $\sim 5 \times 10^{-10}/\mu T$, and thus requires a total field stability of roughly 20 nT to ensure a clock stability of 10^{-11}. This puts stringent requirements on the shielding of the CSAC from external fields. To prevent shifts due to varying orientations of the clock in the earth field ($\pm$ 100 μT), a shielding factor at around 1000 is required. Furthermore, the current of the heaters has to remain constant to within 2 mA (if the field produced by the heaters is perpendicular to the offset field) and 200 μA (if the heater field is parallel to the offset field). This current stability must also be maintained over the full range of ambient temperatures, which is challenging with our current setup. But we believe that a better thermal shielding to reduce the heater currents, higher heater resistances, and nonmagnetic heaters could easily solve this problem. A much better thermal design of the CSAC physics package has been demonstrated for example by Lutwak et al.[9], and could greatly reduce these shifts. Transparent microfabricated heaters with much lower magnetic fields have been developed for chip-scale magnetometers, for example[25], and could be useful in MEMS clocks as well. Better magnetic shielding seems possible by adding a second layer shield and a by use of a better shield design. Finally, MEMS heat switches have been developed with variable thermal resistances, to limit the range of heating currents required[26]. Therefore, the problem of the

long-term clock frequency stability due to magnetic fields could most likely be solved by better engineering of the physics package.

6. OTHER EFFECTS

Although the temperature stabilities of VCSEL and cell and the magnetic fields are currently the biggest contributors to the long-term drifts of our chip-scale atomic clocks, there are other effects that might influence the frequency. One major problem of the VCSELs we use is caused by the presence of a laser mode with polarization orthogonal to the main mode of oscillation. Use of a linear polarizer before the quarter waveplate, aligned with the strong polarization mode of the VCSEL, reduces the effect on the CPT resonance. Nevertheless, we found that mode-competition noise[27, 28] between the two modes can severely degrade the signal-to-noise ratio of the clock resonance, when the polarizer converts polarization fluctuations into amplitude noise on the photodetector. The strength of this effect depends on the individual VCSEL used as well as its particular operating parameters. One method to reduce this additional noise has been demonstrated by Gerginov et al.[29], where one half of the laser beam was circularly polarized and the other half linearly polarized. Both were passed though the same vapor cell and were detected on similar photodetectors. Only the circularly polarized beam caused a CPT resonance, but both had similar AM noise, as a result of FM, AM, and polarization noise converted into amplitude fluctuations by the polarizer and the atomic absorption profile. The difference between the two photodetector signals showed a CPT with much reduced noise.

Many studies have been performed on the lifetimes of VCSELs. Nevertheless, aging effects of VCSELs in such spectroscopic applications and microfabricated alkali vapor cells are largely unknown. In commercial Rb vapor cell clocks, the diffusion of helium into the vapor cells is a major contributor to long-term frequency drifts [30, 31]. While this is often a linear drift in time and can be accounted for in a large device, a low-cost CSAC might not have such sophisticated controls. Helium causes a shift to the Rb clock frequency of 1×10^{-7}/Torr [32]. With the diffusion coefficients of helium through Pyrex measured by F. Norton[33], this would translate into a clock frequency shift of $\sim 3 \times 10^{-11}$/day, assuming pure diffusion through the 200 μm thick Pyrex™† windows of a microfabricated vapor cell of volume 1 mm^3 at 100 °C and natural abundance of He on the outside. The fact that this is very close to the long-term drift we measured in such vapor cells of 5×10^{-11}/day[16] is very surprising, since the actual pressure difference of helium is unknown and no diffusion through the silicon body of the cell, or the anodic bonds have been taken into account. In order to study this effect more precisely, long-term tests should be performed in a controlled helium environment. Furthermore, better thermal design of the heaters and possible Rb reservoirs in the cells might be needed to ensure that the solid metal remains in a desired area of the cell and that no frequency shifts occur from a film of Rb building up on the windows, thus causing changes in the transmission of light through the cell.

7. CONCLUSIONS

We have investigated some major effects that currently limit the long-term frequency stability of our microfabricated atomic clocks. Most of these relate to environmental effects such as temperature variations. Even though strong shifts in the output frequency of our devices are possible, these shifts could be reduced to a large extent by better thermomechanical designs of the physics package and the local oscillator, which may be enabled by MEMS packaging techniques. Primary parameters affecting the output frequency include the temperatures of the vapor cell and the VCSEL, RF output power of the local oscillator, and local magnetic field. Because it could be challenging to reach frequency stabilities of 10^{-11} over integration periods longer than 1 hour and an ambient temperature range of more than 70 °C with pure engineering, we discuss various ideas on how to relax these engineering constraints by implementing atom-based stabilization schemes. However, we have not found effects that in principle would make a CSAC with a frequency stability of 10^{-11} beyond 1 hour impossible.

† Trade name is stated for technical clarity and does not imply endorsement by NIST. Products from other manufacturers may perform as well or better.

ACKNOWLEDGEMENTS

We thank the Microsystems Technology Office of the U.S. Defense Advances Research Program Agency for financial support. A. Brannon is grateful for funding from a graduate research fellowship from the National Science Foundation. This work is a contribution of NIST, an agency of the U.S. government, and is not subject to copyright.

REFERENCES

1. J. Kitching, S. Knappe, and L. Hollberg, "Miniature vapor-cell atomic-frequency references," *Appl. Phys. Lett.*, **81**, 553-555 (2002).
2. M. A. Sturza, "GPS navigation using three satellites and a precise clock," *Global Positioning System*. vol. 2 Washington, DC: Institute of Navigation, 1984, pp. 122-132.
3. J. R. Vig, "Military applications of high accuracy frequency standards and clocks," *IEEE Trans. Ultrason. Ferroelectr. Freq. Control*, **40**, 522-527 (1993).
4. H. Fruehauf, "Fast "direct-P(Y)" GPS signal acquisition using a special portable clock," *Proc. 33rd Ann. Precise Time and Time Interval (PTTI) Meeting*, Long Beach, 2001, pp. 359-369.
5. J. Murphy and T. Skidmore, "A low-cost atomic clock: impact on the national airspace and GNSS availability," *Proceedings of ION GPS-94; 7th International Meeting of the Satellite Division of the Institute of Navigation*, Salt lake City, UT, 1994, pp. 1329-1336.
6. L. A. Liew, S. Knappe, J. Moreland, H. Robinson, L. Hollberg, and J. Kitching, "Microfabricated alkali atom vapor cells," *Appl. Phys. Lett.*, **84**, 2694-2696 (2004).
7. S. Knappe, V. Shah, P. D. D. Schwindt, L. Hollberg, J. Kitching, L. A. Liew, and J. Moreland, "A microfabricated atomic clock," *Appl. Phys. Lett.*, **85**, 1460-1462 (2004).
8. S. Knappe, P. D. D. Schwindt, V. Shah, L. Hollberg, J. Kitching, L. Liew, and J. Moreland, "A chip-scale atomic clock based on Rb-87 with improved frequency stability," *Opt. Express*, **13**, 1249-1253 (2005).
9. R. Lutwak, J. Deng, W. Riley, M. Varghese, J. Leblanc, G. Tepolt, M. Mescher, D. K. Serkland, K. M. Geib, and G. M. Peake, "The Chip-Scale Atomic Clock – Low-Power Physics Package," *Proceedings of the 36th Annual Precise Time and Time Intervals Systems and Applications Meeting*, Washington, DC, 2004, pp. 339-354.
10. R. Lutwak, P. Vlitas, M. Varghese, M. Mescher, D. K. Serkland, and G. M. Peake, "The MAC - A Miniature Atomic Clock," in *Joint Meeting of the IEEE International Frequency Control Symposium and the Precise Time and Time Interval (PTTI) Systems and Applications Meeting* Vancouver, Canada, 2005.
11. A. Brannon, J. Breitbarth, and Z. Popović, "A Low-Power Low Phase Noise Local Oscillator for Chip-Scale Atomic Clocks," *2005 IEEE MTT-S Int. Microwave Symp* 2005.
12. S. Romisch and R. Lutwak, "Low-Power, 4.6-GHz Stable Oscillator for CSAC " *International Frequency Control Symposium*, Miami, FL, 2006.
13. A. Brannon, M. Janković, J. Breitbarth, Z. Popović, V. Gerginov, V. Shah, S. Knappe, L. Hollberg, and J. Kitching, "A Local Oscillator for Chip-Scale Atomic Clocks at NIST," *IEEE Frequency Control Symposium*, Miami, FL, 2006, in press.
14. A. Brannon, V. Gerginov, S. Knappe, Z. Popović, and J. Kitching, "A miniature atomic clock for GPS," *in preparation*, (2006).
15. G. Alzetta, A. Gozzini, L. Moi, and G. Orriols, "Experimental-Method for Observation of Rf Transitions and Laser Beat Resonances in Oriented Na Vapor," *Nuovo Cimento Della Societa Italiana Di Fisica B-General Physics Relativity Astronomy and Mathematical Physics and Methods*, **36**, 5-20 (1976).
16. S. Knappe, V. Gerginov, P. D. D. Schwindt, V. Shah, H. Robinson, L. Hollberg, and J. Kitching, "Atomic vapor cells for chip-scale atomic clocks with improved long-term frequency stability," *Opt. Lett.*, **30**, 2351-2353 (2005).
17. M. Arditi and T. R. Carver, "Pressure, Light, and Temperature Shifts in Optical Detection of 0-0 Hyperfine Resonance of Alkali Metals," *Physical Review*, **124**, 800 (1961).

18. J. Vanier, R. Kunski, N. Cyr, J. Y. Savard, and M. Tetu, "On Hyperfine Frequency-Shifts Caused By Buffer Gases - Application To The Optically Pumped Passive Rubidium Frequency Standard," *J. Appl. Phys.*, **53**, 5387-5391 (1982).
19. V. Gerginov, V. Shah, S. Knappe, L. Hollberg, and J. Kitching, "Atomic-based stabilization for laser-pumped atomic clocks," *Opt. Lett.*, **31**, 1851-1853 (2006).
20. M. Zhu and L. S. Cutler, "Theoretical and experimental study of light shift in a CPT-based Rb vapor cell frequency standard," *Proceedings of the 32nd Annual Conference on Precise Time and Time Interval Systems and Applications Meeting*, Reston, VA., 2000, pp. 311-324.
21. J. Vanier, A. Godone, and F. Levi, "Coherent microwave emission in Coherent Population Trapping: Origin of the energy and of the quadratic light shift," *Proceedings of the Annual IEEE International Frequency Control Symposium*, 1999, pp. 96-99.
22. F. Levi, A. Godone, and J. Vanier, "Light shift effect in the coherent population trapping cesium maser," *IEEE Transactions on Ultrasonics, Ferroelectrics, and Frequency Control*, **47**, 466-470 (2000).
23. V. Gerginov, S. Knappe, V. Shah, P. D. D. Schwindt, L. Hollberg, and J. Kitching, "Long-term frequency instability of atomic frequency references based on coherent population trapping and microfabricated vapor cells," *J. Opt. Soc. Am. B-Opt. Phys.*, **23**, 593-597 (2006).
24. V. Shah, V. Gerginov, P. D. D. Schwindt, S. Knappe, L. Hollberg, and J. Kitching, "Continuous Light Shift Correction in Modulated CPT Clocks," *Appl. Phys. Lett.*,**89**, 151124 (2006).
25. P. D. D. Schwindt, B. Lindseth, S. Knappe, V. Shah, and J. Kitching, "A chip-scale atomic magnetometer with improved sensitivity using the Mx technique," *Appl. Phys. Lett.*, (2006).
26. A. Laws, R. Y. J. Chang, V. M. Bright, and Y. C. Lee, "Thermal management for chip-scale atomic clocks," *Proceedings of the ASME/Pacific Rim Technical Conference and Exhibition on Integration and Packaging of MEMS, NEMS, and Electronic Systems: Advances in Electronic Packaging 2005*, 2005, pp. 741-746.
27. T. Mukaihara, N. Ohnoki, Y. Hayashi, N. Hatori, F. Koyama, and K. Iga, "Excess intensity noise originated from polarization fluctuation in vertical-cavity surface-emitting lasers," *Photonics Technology Letters, IEEE*, **7**, 1113-1115 (1995).
28. J. Kaiser, C. Degen, and W. Elsaässer, "Polarization-switching influence on the intensity noise of vertical-cavity surface-emitting lasers," *Journal of the Optical Society of America B: Optical Physics*, **19**, 672-677 (2002).
29. V. Gerginov, S. Knappe, V. Shah, L. Hollberg, and J. Kitching, "Laser noise cancellation in single-cell CPT clocks," *In preparation* (2006).
30. M. Bloch, O. Mancini, and T. McClelland, "Performance of rubidium and quartz clocks in space," *2000 IEEE Frequency Control Symposium*, 2000, pp. 505-509.
31. J. C. Camparo, C. M. Klimcak, and S. J. Herbulock, "Frequency equilibration in the vapor-cell atomic clock," *IEEE Trans. Instrum. Meas.*, **54**, 1873-1880 (2005).
32. P. L. Bender, E. C. Beaty, and A. R. Chi, "Optical Detection of Narrow Rb^{87} Hyperfine Absorption Lines," *Phys. Rev. Lett.*, **1**, 311 (1958).
33. F. J. Norton, "Permeation of Gases through Solids," *J. Appl. Phys.*, **28**, 34-39 (1957).